ANNUAL REPORT 2007

Statistics of Ground Motions in a Physical System

Matthew Purvance, John Anderson, Rasool Anooshehpoor, James Brune
Seismological Laboratory, University of Nevada, Reno

INTRODUCTION

Brune (1973) pioneered the use of foam rubber to investigate the characteristics of dynamic ruptures in a physical system. Foam rubber models have provided valuable insights into earthquake predictability and triggering (Brune et al., 1989), fault normal vibrations and associated slip pulses (Brune et al., 1989; Brune et al., 1993; Anooshehpoor and Brune, 1994), and the lack of frictional heat production during dynamic stick-slip events (Anooshehpoor and Brune, 1994). Previous SCEC funding has been used to record and analyze ~1,400 foamquakes in the strike-slip model (Figure 1) to delineate the particle motion distributions produced by dynamic ruptures in this analog model of an earthquake fault. The strike-slip model consists of two ~ meter sized foam blocks driven past one another via a hydraulic piston. The foam blocks have been instrumented with 64 piezoelectric accelerometers and 6 displacement sensors. We have increased the number of recorded and analyzed events to greater than 6,800, approaching the stated goal of 10,000 events recorded and analyzed in this model. This report documents initial work related to describing the statistical characteristics of the particle motion distributions with special attention paid to the largest amplitude motions.

GROUND MOTION DISTRIBUTIONS

The strike-slip foam rubber model produces three distinct styles of rupture, namely Mode II forward ruptures (MIIF), Mode II backward ruptures (MIIB), and Mode III ruptures (MIII) (Figure 2). These various rupture styles occur in spite of the fact that the rupture surface is smooth on scales greater than about a centimeter. 64% of the recorded ruptures are MIIF, nucleating on the side of the model with the driving piston (the "back"), while only 22% of the ruptures are MIIB (nucleating near the "front" of the model) and 14% are MIII (nucleating near the "bottom" of the model). In terms of predictability of rupture style, 87% of MIIF ruptures are immediately preceded by MIIF ruptures, while 64% of MIIB ruptures are preceded by MIIB ruptures and 33% of MIII ruptures are immediately preceded by MIII ruptures. Should the rupture styles be randomly distributed with order, the percentages of rupture pairs of the same style would be similar to their total proportion, demonstrating that the rupture styles of adjacent events are indeed well correlated.

The remainder of this preliminary work focuses on the particle motion distributions measured on the "side" of the model which is equivalent to the surface of the earth. The fault-parallel particle motion distributions at an array of sensors are shown in Figure 3. Both the MIIF and MIIB particle distributions demonstrate significant directivity, with the forward directivity sensors experiencing an approximate three-fold increase in particle velocity. Figure 4 presents the stacked motion distributions for each rupture mode and for fault parallel/perpendicular PGA and PGV. Stacking refers to the total particle motion distributions using all sensors with identical distances to the rupture

surface (e.g., identical Boore-Joyner distances - ~ 47,000 total measurements). This sort of stacking is a common practice in the determination of ground motion prediction equations (GMPE) from recorded ground motions. Notice that the MIIB and MIII stacked distributions are nearly identical. In addition, the MIIF particle motion distributions demonstrate long, high amplitude tails corresponding to relatively rare measurements of very high particle motions; these long tails are the result of very strong directivity events. We have applied the Kolmogorov-Smirnov test to determine with what probabilities both the stacked and single sensor particle motion distributions are indistinguishable from lognormal. This work finds that the particle motion distributions are all indistinguishable from lognormal with less than 1% probability. In other words, there is less than 1 chance in 100 that the ground motion distributions are lognormal. These findings highlight the fact that the shapes of the distributions as determined from central portions of the distributions (from the mean and standard deviations) do not represent the statistical properties of the tails.

In order to investigate the statistical characteristics of the tails of the particle motion distributions, we have applied a method commonly used to determine structural loads from extreme wind speeds. de Haan (1994) describes the point over threshold method which tests the tails of a distribution for consistency with one of three different forms of the generalized Pareto distribution. The generalized Pareto distribution is given by

$$G(y) = \begin{cases} 1 - \left(1 - \dfrac{c(y-h)}{a}\right)^{1/c}, c \neq 0 \\ 1 - \exp\left(-\dfrac{y-h}{a}\right), c = 0 \end{cases}$$

where h is a location parameter, a is an amplitude parameter, and c is a shape parameter. The parameter c is of particular significance as differing values of this parameter signify different distributions with significantly different properties with regards to the tails. For $c > 0$, the distribution is unbounded and termed a Frechet distribution. For $c = 0$, the distribution is exponential and termed a Gumbel distribution. For $c < 0$, the distribution is bounded and is termed a reverse Weibull distribution. Estimates of the parameter c vary with the threshold chosen for the analysis as the method examines the statistical properties of the number of observations above the specified threshold. Figure 5 presents estimates of c for the fault parallel/perpendicular PGA and PGV values. As the thresholds are lowered form the most extreme possible values, $c < 0$ in all cases. This suggests that the particle motion distributions are most consistent with the reverse Weibull distribution and are thus bounded.

CONCLUSIONS

This report highlights some of the major results that we have obtained recently from the foam rubber rupture model. With over 6,800 events recorded to date, we are approaching the goal of recording 10,000 events. This work demonstrates that the rupture styles are well correlated in time and that the particle motion distributions are not consistent with lognormal distributions. In fact, the tails of the particle motion distributions are most consistent with the reverse Weibull distribution which is bounded. The ramifications of using such a bounded ground motion distribution for probabilistic

seismic hazard analysis are that the predicted ground motion amplitudes are bounded. In other words, as one goes to lower and lower probabilities of exceedences, the ground motions amplitudes do not increase forever unlike for the case of assuming lognormal ground motion distributions. These results are very important for sensitive structures for which one requires estimates of the seismic hazard over very long time periods.

REFERENCES

Anooshehpoor, A., and J. N. Brune. (1994) "Frictional Heat Generation and Seismic Radiation in a Foam Rubber Model of Earthquakes," *PAGEOPH*, *142*, 735-747.

Brune J. N. (1973) "Earthquake Modeling by Stick-Slip along Pre-Cut Surfaces in Stressed Foam Rubber, *Bull. Seism. Soc. Am.*, *63*, 2105-2119.

Brune, J. N., S. Brown and P. A. Johnson. (1993) "Rupture Mechanism and Interface Separation in Foam Rubber Models of Earthquakes: A Possible Solution to the Heat Flow Paradox and the Paradox of Large Overthrusts," *Tectonophysics*, *218*, 59-67.

Brune, J. N., P. A. Johnson and C. Slater. (1989) "Constitutive Relations for Foam Rubber Stick-Slip," *Seis. Res. Lett.*, *60*, 26.

de Haan. Extreme value statistics. In: Galambos J, Lechner JA, Simiu E, editors. Extreme value theory and applications. Dordrecht: Kluwer Academic Publishers, 1994.

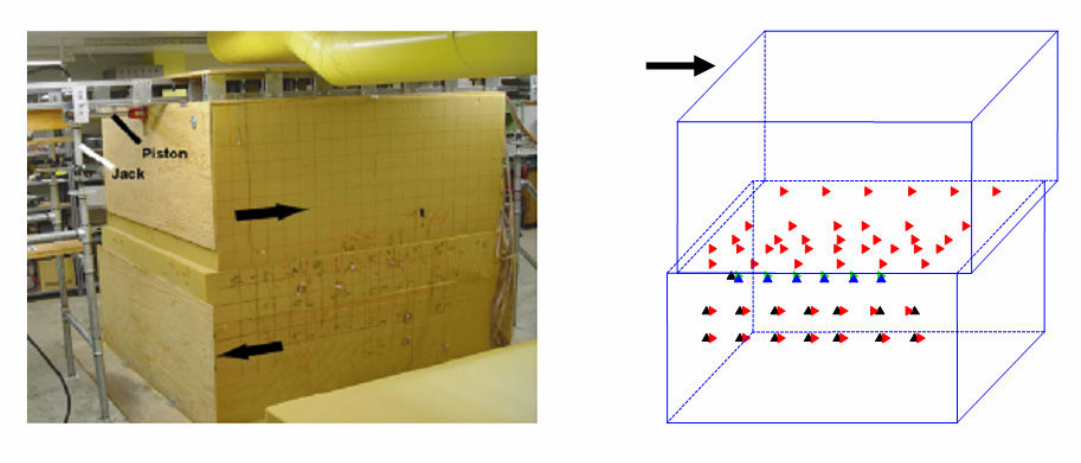

Figure 1. Left: Picture of the strike-slip rupture model constructed of foam rubber. Right: Instrumental layout of accelerometers (red and black) and displacement sensors (blue and green). The front face is similar to the surface of the earth.

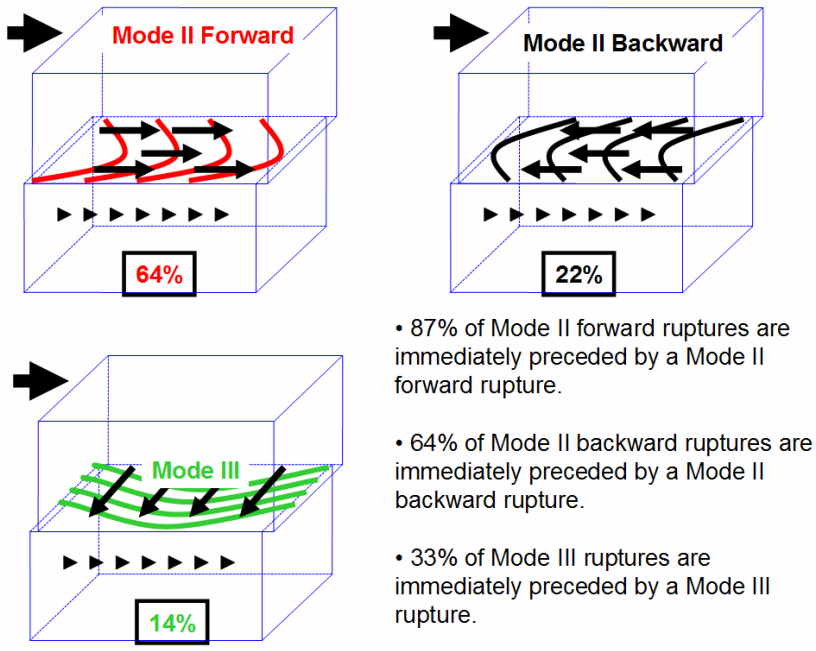

Figure 2. Styles of rupture. Upper left: MIIF; upper right: MIIB; lower left: MIII.

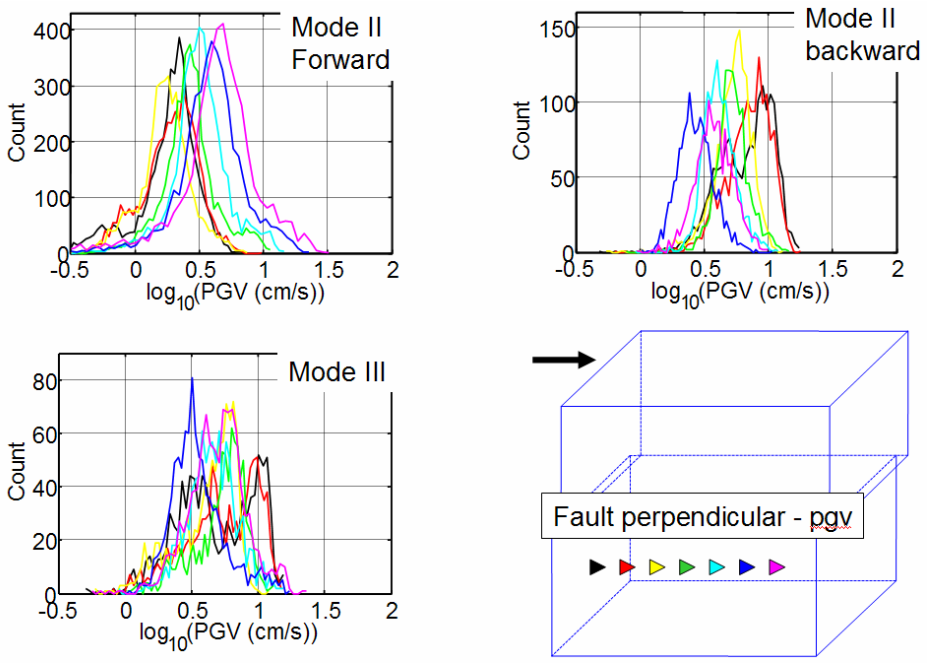

Figure 3. Fault-parallel PGV as a function of sensor locations for the three different rupture styles. The traces are color coded by the key given at the bottom right. Notice the clear signs of directivity in the MIIF and MIIB events (upper left and right, respectively).

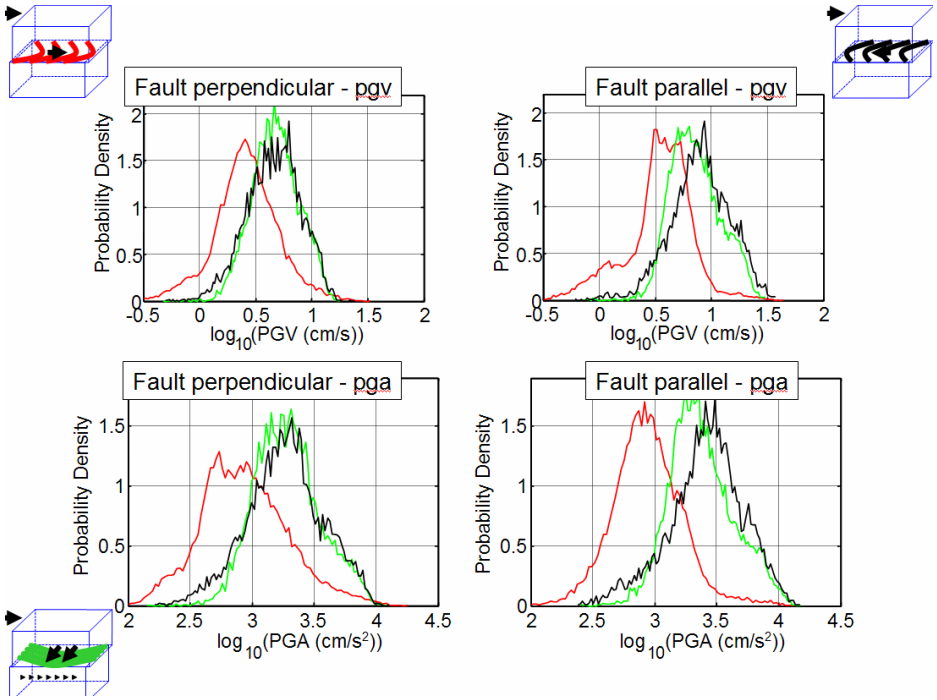

Figure 4. Stacked particle motion distributions for fault parallel/perpendicular PGA and PGV. The colors represent the various rupture styles: red = MIIF, black = MIIB, and green = MIII.

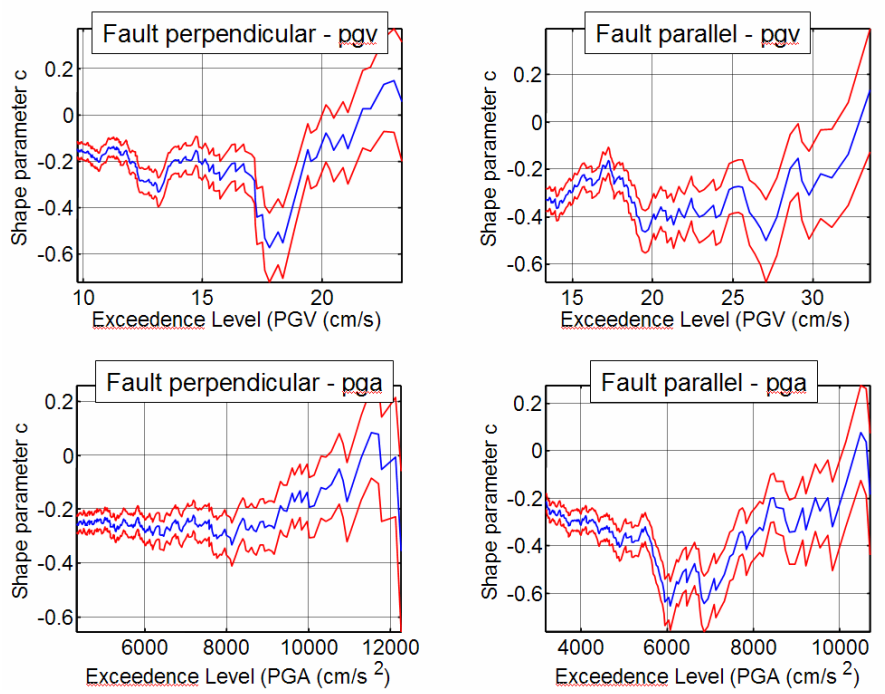

Figure 5. Shape parameters *c* (blue lines) as determined from the point over threshold method as a function of the threshold level (e.g., exceedence level) for fault parallel/perpendicular PGA and PGV. Red lines represent the ± 1σ counds on *c*.